ICES Journal of Marine Science

ICES Journal of Marine Science (2016), 73(3), 680–692. doi:10.1093/icesjms/fsv259

Contribution to Special Issue: 'Towards a Broader Perspective on Ocean Acidification Research'

Original Article

Effects of high CO_2 levels on the ecophysiology of the diatom *Thalassiosira weissflogii* differ depending on the iron nutritional status

Koji Sugie*‡ and Takeshi Yoshimura

Central Research Institute of Electric Power Industry, 1646 Abiko, Abiko, Chiba 270-1194, Japan

**Corresponding author. tel: +81 46 867 9449; fax: +81 46 867 9455; e-mail: sugie@jamstec.go.jp*
‡*Present address: Research and Development Center for Global Change, Japan Agency for Marine-Earth Science and Technology, 2-15, Natsushima-cho, Yokosuka, Kanagawa 233-0061, Japan.*

Sugie, K., and Yoshimura, T. Effects of high CO_2 levels on the ecophysiology of the diatom *Thalassiosira weissflogii* differ depending on the iron nutritional status. – ICES Journal of Marine Science, 73: 680–692.

Received 23 April 2015; revised 7 December 2015; accepted 8 December 2015; advance access publication 6 January 2016.

Iron availability in seawater, namely the concentration of dissolved inorganic iron ([Fe′]), is affected by changes in pH. Such changes in the availability of iron should be taken into account when investigating the effects of ocean acidification on phytoplankton ecophysiology because iron plays a key role in phytoplankton metabolism. However, changes in iron availability in response to changes in ocean acidity are difficult to quantify specifically using natural seawater because these factors change simultaneously. In the present study, the availability of iron and carbonate chemistry were manipulated individually and simultaneously in the laboratory to examine the effect of each factor on phytoplankton ecophysiology. The effects of various pCO_2 conditions (~390, ~600, and ~800 μatm) on the growth, cell size, and elemental stoichiometry (carbon [C], nitrogen [N], phosphorus [P], and silicon [Si]) of the diatom *Thalassiosira weissflogii* under high iron ([Fe′] = ~240 pmol l^{-1}) and low iron ([Fe′] = ~24 pmol l^{-1}) conditions were investigated. Cell volume decreased with increasing pCO_2, whereas intracellular C, N, and P concentrations increased with increasing pCO_2 only under high iron conditions. Si:C, Si:N, and Si:P ratios decreased with increasing pCO_2. It reflects higher production of net C, N, and P with no corresponding change in net Si production under high pCO_2 and high iron conditions. In contrast, significant linear relationships between measured parameters and pCO_2 were rarely detected under low iron conditions. We conclude that the increasing CO_2 levels could affect on the biogeochemical cycling of bioelements selectively under the iron-replete conditions in the coastal ecosystems.

Keywords: diatoms, elemental composition, iron availability, nutrients, ocean acidification, *Thalassiosira weissflogii*.

Introduction

Ongoing increases in CO_2 in seawater resulting from anthropogenic activities affect carbonate chemistry and result in a decrease in pH and an increase in the partial pressure of CO_2 (pCO_2; i.e. ocean acidification; Doney *et al.*, 2009). The effect of changing carbonate chemistry on phytoplankton has attracted much research attention over the last decade. Because phytoplankton is a crucial component of the marine ecosystem, understanding the effects of ocean acidification on phytoplankton processes is important to predict the future health of the marine ecosystem (Doney *et al.*, 2009; IGBP, IOC, and SCOR, 2013).

The bioavailability of trace metals is affected by changing carbonate chemistry, which in turn affects the relationship between trace metals and pH-sensitive inorganic/organic coordination chemistry (Millero *et al.*, 2009). Shi *et al.* (2010) reported that the conditional stability constant of iron–organic ligand complexes increased as pH decreased when the ligand was an acidic binding group. Previous CO_2 perturbation studies have indicated that iron availability can decrease in low pH–high CO_2 conditions (Shi *et al.*, 2010; Sugie *et al.*, 2013), but the results may largely depend on the sensitivity of each phytoplankton community to changes in iron availability

(Sugie *et al.*, 2013; Yoshimura *et al.*, 2013, 2014). In addition, the chemical nature of iron-binding ligands in natural seawater is largely uncertain. Such uncertainty implies that simultaneous changes in carbonate chemistry and iron availability in natural seawater make it difficult to discriminate the effect of each factor on phytoplankton ecophysiology. To properly interpret the results of ocean acidification studies in the natural environment, it is necessary to understand the individual effects of changes in carbonate chemistry and iron availability on phytoplankton ecophysiology.

Iron has important roles in the metabolism of phytoplankton such as photosynthesis, nitrogen (N) assimilations, and respiration (Raven *et al.*, 1999). One of the most bioavailable form of iron for eukaryotic phytoplankton is dissolved inorganic iron (Fe′) species mainly composed of $Fe(OH)_2^+$, $Fe(OH)_4^-$, and $Fe(OH)_3^0$ in seawater (Morel *et al.*, 2008). In contrast, iron uptake from iron–organic ligand complex is often a very slow process for eukaryotes, indicating that such complex shows low iron bioavailability. Therefore, to investigate the effect of iron availability on phytoplankton processes, Fe′ rather than total iron in seawater must be considered. The binding affinities of iron with ethylene diamine tetraacetic acid (EDTA) and with bacterial hydroxamate siderophore desferrioxamine B are sensitive to changes in seawater pH (Shi *et al.*, 2010). For example, 100 μmol l^{-1} EDTA bound with 100 nmol l^{-1} ferric iron under 20°C and 100 μmol photon m^{-2} s^{-1}, 12:12 h light:dark conditions was used to demonstrate that a decrease in pH from 8.0 to 7.8 potentially decreased the concentration of Fe′ ([Fe′]) from 90 to 26 pmol l^{-1} (Sunda and Huntsman, 2003). Recently, Sugie and Yoshimura (2013) demonstrated that a combination of iron, EDTA, and CO_2 concentration-controlled air can be used to manipulate [Fe′] and carbonate chemistry separately and simultaneously. However, most previous studies did not discriminate the effects of changes in iron availability from changes in carbonate chemistry.

Dissolved iron (<0.2 μm) concentrations in coastal waters (>~1 nmol l^{-1}) are generally higher and more spatio-temporally dynamic than that of oceanic waters (<~0.5 nmol l^{-1}; Kuma *et al.*, 2000; Nishioka *et al.*, 2013). The dynamic nature of dissolved iron concentrations in coastal environment reflects the iron sources, and physical and chemical properties of seawater. For example, riverine inputs and vertical mixing involving sediments could increase iron concentrations, whereas intrusion of oceanic waters and the low solubility of Fe′ in seawater could decrease the concentrations (Kuma *et al.*, 2000). Furthermore, one of the most important factors determining dissolved iron concentrations is the concentration and binding affinity (Log $K^{Cond}_{FeL,Fe'}$) of organic ligands (Kuma *et al.*, 2000; Bundy *et al.*, 2015). Therefore, iron bioavailability, namely the [Fe′], could dynamically change depending on the organic and inorganic chemistry of seawater.

Iron requirement is generally higher in coastal phytoplankton species than in oceanic species, probably reflecting the environmental conditions of their habitats (e.g. Sunda and Huntsman, 1995). As a result, the effects of changes in iron availability with changes in CO_2 conditions could differ depending on the nature of the iron requirement of each phytoplankton species. One of the notable effects of iron availability on phytoplankton is change in the elemental composition of diatoms (e.g. Takeda, 1998). Changes in CO_2 concentrations can also alter the cellular elemental composition of diatoms (e.g. Sun *et al.*, 2011; Sugie and Yoshimura, 2013), indicating that changes in either iron availability or CO_2 concentration could affect marine biogeochemical cycling of bioelements. However, other than the study by Sugie and Yoshimura (2013), no studies have demonstrated the individual effects of iron availability and CO_2 conditions on the elemental composition of phytoplankton. Because the response to the changes in iron availability and CO_2 variations differ among species (Burkhardt *et al.*, 1999; Doney *et al.*, 2009; Bucciarelli *et al.*, 2010), more studies on the elemental composition of phytoplankton are needed to better understand the biogeochemistry of the ocean.

To date, prediction of future environments has relied on *in silico* simulations. One of the major problems in estimating biogeochemical cycling of bioelements in modelling studies is the behaviour of the elemental composition of phytoplankton, which is usually fixed as the canonical Redfield ratio (Passow and Carlson, 2012). In forecasts on global and long-time-scales, Redfield ratio-based simulation is assumed to be representative of the nutrient budget in the ocean. However, models simulating changes on regional, and short-time-scales should consider the flexible elemental composition of phytoplankton to represent the ecological stoichiometry in dynamic environments (Smith *et al.*, 2011; Passow and Carlson, 2012). Quigg *et al.* (2003) reported that individual phytoplankton taxa have unique elemental stoichiometry. The regional characteristics of elemental composition of marine particulate matter therefore reflect the elemental stoichiometry of dominant phytoplankton taxa (Weber and Deutsch, 2010). Similarly, changes in the elemental composition of phytoplankton communities in response to environmental changes differ among reports, probably as a result of differences in the community composition (Sugie *et al.*, 2013; Eggers *et al.*, 2014; Richier *et al.*, 2014; Yoshimura *et al.*, 2014). Therefore, more information is needed on species-specific differences in the effects of environmental disturbances on the ecophysiology of phytoplankton.

Here, we examine the individual effects of carbonate chemistry and iron availability on the elemental composition (carbon [C], [N], phosphorus [P], and silicon [Si]) of estuarine and coastal diatom *Thalassiosira weissflogii*. In addition to the dynamics of iron, coastal and estuarine systems are also more dynamic in terms of carbonate chemistry than oceanic systems (Wootton *et al.*, 2008; Dore *et al.*, 2009). This study can provide useful information about first-order biogeochemical processes of nutrients in neritic ecosystems.

Material and methods

Experimental set-up

Seawater used for the experiment (salinity 34.2) was collected from a coastal region in the North Pacific, near Onjuku, Chiba, Japan (35°18′N, 140°38′E). About 50 l of seawater was filtered through a 0.22-μm cartridge filter (Advantech Co. Ltd, Tokyo, Japan). Stock solutions of macronutrients were passed through a Chelex 100 resin (Bio-Rad, CA, USA) to eliminate trace metals (Price *et al.*, 1988/1989), and then added to the filtered seawater to make final concentrations of ~100 μmol l^{-1} NO_3^-, ~6 μmol l^{-1} PO_4^-, and ~150 μmol l^{-1} $Si(OH)_4$. The seawater with added nutrients was aged for more than 1 month in an acid-washed 50-l polypropylene carboy, to precipitate dissolved iron excess to its solubility (Sugie *et al.*, 2010; Sugie and Yoshimura, 2013). The aged seawater was passed through a 0.1-μm cartridge filter (Merck Millipore, MA, USA) to sterilize it and to eliminate particulate iron before use. The background iron concentration of the filtered seawater was 0.4 nmol l^{-1}, as measured by flow-injection with chemiluminescence detection (Obata *et al.*, 1993). The culture medium used in this study was modified Aquil medium (Price *et al.*, 1988/1989), which was composed of nutrient-enhanced 0.1 μm filtered seawater and Aquil metals chelated with 100 μmol l^{-1} of EDTA. Only iron

concentrations were modified during the culture experiment. An algal strain of *T. weissflogii* (Grunow) G. Fryxell and Hasle [currently accepted as *Conticribra weissflogii* (Grunow) K. Stachura-Suchoples and D.M. Williams; CCMP1336] was maintained in modified Aquil medium at 20°C under cool fluorescent light at 150 μmol photons m^{-2} s^{-1} (measured using QSL radiometer; Biospherical Instrument Inc., CA, USA), and a 12:12 h light:dark cycle. All equipment used in the culture experiment was acid-washed (soaked for at least 24 h in either 1 or 4 mol l^{-1} HCl solution) followed by thorough rinsing with Milli-Q water (>18.0 MΩ cm^{-1}, Merck KGaA, Darmstadt, Germany). Preparation and sampling were conducted in a class 1000 clean room and at a class 100 clean bench, respectively, to avoid inadvertent trace metal contamination.

Culture design

Iron, other trace metals, and EDTA stock solutions were mixed and left for ~1 h in 4-l polycarbonate culture bottles before pouring 3-l of nutrient-enhanced 0.1-μm filtered seawater. Next, CO_2 concentration (xCO_2)-controlled air (Nissan Tanaka Corp., Saitama, Japan) was injected to manipulate the carbonate chemistry of the culture medium. The xCO_2 of the injected air was set at 386, 614, or 795 ppm, corresponding to the present and two possible future CO_2 conditions, respectively, and these high CO_2 conditions could also be found in the present coastal region during winter (Wootton *et al.*, 2008). The injected air was humidified by passing through Milli-Q water and it was also passed through a 0.2 μm inline filter to avoid contaminations from the gas cylinder or lines. The flow rate of xCO_2-controlled air was set at 40 ml min^{-1} for 4 d before the start of the experiment to ensure steady state of carbonate chemistry and to equilibrate [iron–EDTA], [EDTA], and [Fe′] conditions. The [Fe′] was set at 30 or 250 pmol l^{-1} for low iron (LFe) and high iron (HFe) treatments, respectively. The values for [Fe′] were determined based on a presurvey of the relationship between specific growth rates and [Fe′] (Figure 1). Non-linear fitting of the growth rate and [Fe′] data to the Monod equation, resulted in a maximum specific growth rate (μ_{max}) = 1.24 ± 0.04 (d^{-1}) and a half saturation constant for growth (k_μ) = 28.1 ± 3.2 (pmol l^{-1}) ($R^2 = 0.98$, $p < 0.001$). The [Fe′] of 30 and 250 pmol l^{-1} were selected to produce ~50 and >90% of the μ_{max} of *T. weissflogii*, respectively. In coastal seawater, given the dissolved iron and iron-binding ligand concentrations of 1–150 and 10–500 nmol l^{-1}, respectively, with (Log $K^{Cond}_{FeL,Fe'}$) of ligands ranging 8.7–12 (Kuma *et al.*, 2000; Laglera and van den Berg, 2009; Hassler *et al.*, 2011; Bundy *et al.*, 2015), the [Fe′] could range from 0.1 to 297 pmol l^{-1}. Given these iron conditions and the dynamics of carbonate chemistry in the coastal region, this study could partially simulates the present coastal environment as well as future high CO_2 conditions. Six treatments based on different xCO_2 and [Fe′] were established as follows: LFe386, LFe614, LFe795, HFe386, HFe614, and HFe795. When estimating [Fe′] according to the method of Sunda and Huntsman (2003), the background concentration of iron was included in the added iron concentrations. Defined [Fe′] were obtained using total iron and EDTA concentrations, pH, light intensity and duration, and temperature. The pH values were calculated from measurements of total alkalinity (TA) and dissolved inorganic C (DIC) concentrations (Table 1). Cultures were set in duplicate bottles for each treatment.

The dilute batch culture technique was used in this study (LaRoche *et al.*, 2011); the diatom cells were harvested <20% of the carrying capacity of the culture medium to avoid large changes in carbonate chemistry and iron availability. To acclimate and to reduce intracellularly stored iron of the *T. weissflogii* cells to experimental conditions, cells in stock culture (exponential growth phase) were transferred to each xCO_2 with 1/100 Aquil trace metals medium and grown in the exponential growth phase corresponding to ~10 cell divisions. The xCO_2-acclimated cells were then transferred to the experimental media to give an initial cell density of 100 and 50 cells ml^{-1} in the LFe- and HFe-treated bottles, respectively. Cultures were continued for 10 and 6 d in the LFe and HFe treatments, respectively, representing 6–7 cell divisions under the experimental conditions. Geider *et al.* (1993) reported that iron-limited diatom cell could acclimate under high-iron conditions within 24 h, and thus, *T. weissflogii* should acclimate each iron conditions during the experiment. After inoculation of the diatoms into the experimental media, the flow rate of xCO_2-controlled air was reduced to 10 ml min^{-1}.

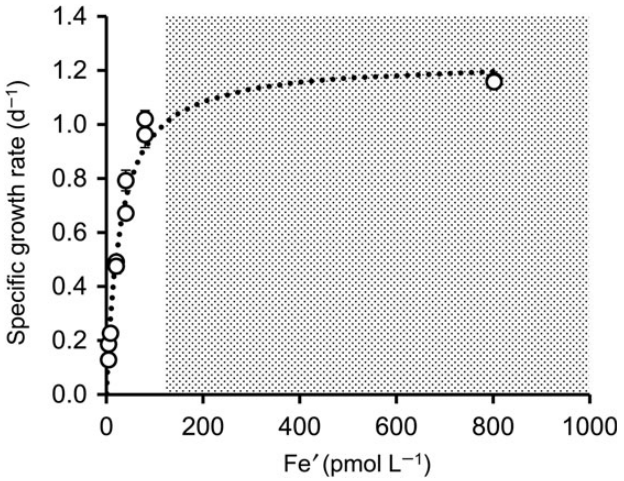

Figure 1. Change in the specific growth rate of *T. weissflogii* against the change in dissolved inorganic iron (Fe′) concentration. The hatched area represents where solid iron hydroxides are precipitating (e.g. Stumm and Morgan, 1996), and therefore [Fe′] may not be correct. The dotted hyperbolic line was obtained by non-linear fitting of the data on the relationship between the specific growth rate of *T. weissflogii* and [Fe′] to the Monod equation.

Measurements

Growth was monitored daily at a fixed time (mid of the light phase) using a Multisizer 4 Coulter Counter (Beckman Coulter Inc., CA, USA) to calculate specific growth rates and to measure cell volume and surface area (SA). Specific growth rates (μ, d^{-1}) were determined from the slope of a plot of the natural log density of biovolume (i.e. abundance × cell volume) against time during the exponential growth phase. At the end of the experiment, cells were harvested on precombusted GF/F filters for particulate organic C (POC), particulate N (PN), and particulate P (PP) analysis. For biogenic Si (BSi) analysis, samples were collected on a 0.8-μm polycarbonate filter. The methods for POC, PN, PP, and BSi measurements have been described elsewhere (Sugie and Yoshimura, 2013). In brief, for POC and PN analysis, filters were freeze-dried, and the concentrations were measured using a CHN analyser. Filters for PP analysis were combusted in high temperature followed by acid hydrolysis and measured using a spectrophotometer as described by Solórzano and Sharp (1980). For BSi analysis, the filter was digested in 0.5% Na_2CO_3 solution (Paasche, 1980) and measured with a QuAAtro-2 continuous flow analyser. For chlorophyll *a*

Table 1. Measured TA (in μmol kg^{-1}) and DIC (in μmol kg^{-1}), and calculated dissolved inorganic iron species (Fe′ in pmol l^{-1}) conditions during the experiment.

	Initial			Day 2 (HFe) or day 3 (LFe)			Day 6 (HFe) or day 9 (LFe)		
Treatment	**TA**	**DIC**	**Fe′**	**TA**	**DIC**	**Fe′**	**TA**	**DIC**	**Fe′**
LFe-386	2344	2087	23.0	2349	2076	26.1	2356	2063	30.7
LFe-614	2353	2161	24.6	2359	2160	25.9	2364	2162	26.8
LFe-795	2350	2196	24.9	2359	2197	26.8	2368	2199	28.5
HFe-386	2351	2113	168*	2352	2081	220*	2365	2047	322*
HFe-614	2357	2164	222*	2355	2157	233*	2364	2145	280*
HFe-795	2353	2200	220*	2354	2193	237*	2363	2185	276*

Data represents mean of the duplicate bottles. Note that the Fe′ concentrations in the HFe treatments with asterisks show an approximate values because the concentrations were over-saturated with respect to the solubility of dissolved inorganic Fe(III) hydroxide (e.g. Stumm and Morgan, 1996).

(Chl *a*) measurements, seawater samples were filtered on GF/F filters, soaked in *N*,*N*-dimethylformamide (Suzuki and Ishimaru, 1990) and quantified by fluorometry (Welschmeyer, 1994). All data for POC, PN, PP, BSi, and Chl *a* concentrations were corrected by subtracting values obtained from filter blanks. The cell quota of each element (Q_E) was calculated by dividing the concentration of each element by abundance. To estimate intracellular concentrations of each element ($In_{cell}[E]$), POC, PN, PP, and Chl *a* concentrations were divided by abundance and cell volume, to obtain $In_{cell}[C]$, $In_{cell}[N]$, $In_{cell}[P]$, and $In_{cell}[Chl\ a]$, respectively. The BSi concentration was normalized by abundance and SA ([Si]/SA) because most BSi localizes outwards as siliceous frustules. Net elemental production (NEP) was calculated as follows: $NEP = Q_E \times \mu$.

The DIC and TA samples were collected and measured at days 0, 2, and 6 for HFe conditions and days 0, 3, and 10 for LFe conditions. Both parameters were measured using a potentiometric Gran plot method with 0.1 mol l^{-1} HCl (Wako Co. Ltd, Osaka, Japan) and a TA analyser (Kimoto Electric Co. Ltd, Osaka, Japan), according to the method of Edmond (1970). Titration data below pH 4 were eliminated because EDTA began absorbing protons below pH ∼4. The stability of the DIC and TA analyses was checked using DIC reference material (KANSO Co. Ltd, Osaka, Japan) and the analytical errors in this study were <0.1% for both DIC (∼1.1 μmol kg^{-1}) and TA (∼1.4 μmol kg^{-1}). The DIC and TA values of the reference material were traceable to the certified reference materials supplied by Professor Andrew Dickson, University of California, San Diego, USA. Carbonate chemistry was calculated using the CO2SYS program and DIC and TA data (Lewis and Wallance, 1998). Samples for macronutrient analysis were collected at the end of the experiment and measured using a QuAAtro-2 continuous flow analyser.

Statistics

Linear regression was used to test the relationship between measured parameters and pCO_2. When significant linearity was found ($p < 0.05$), the regression line was described in the figure. When the hypothesis of linearity was rejected, differences among the different xCO_2 treatments were tested with Tukey's HSD ANOVA test. To test the effect of the different [Fe′] of each of three xCO_2 treatments, two-tailed, paired-sample *t*-tests were performed. All statistics were carried out using PASW statistical software (version 17.0 SPSS Inc., Chicago, IL, USA). Significant differences are reported at the 95% confidence level.

Results

The pH and pCO_2 were clearly different among the xCO_2 tested throughout the experiment with a slight increase in pH and a decrease in pCO_2 during incubations (Figure 2, Table 1). The [Fe′] was not statistically different among the three xCO_2 treatments under both LFe and HFe conditions (Figure 3, Table 1). The specific growth rate differed significantly between the HFe614 and HFe795 treatments, but there was no significant difference in specific growth rate between the HFe386 and HFe614 treatment or between the HFe386 and HFe795 treatment (Figure 4a). Under LFe conditions, the specific growth rate was slightly increased by the change in carbonate chemistry, but the difference was not statistically significant ($p = 0.13$, ANOVA; Figure 4a, Table 2). The cell volume decreased linearly with increasing pCO_2 under HFe conditions (Table 2), whereas no linearity was found under LFe conditions (Figure 4b). Under LFe conditions, there was a significant decrease in the cell volume for the LFe614 treatment compared with the LFe386 and LFe795 treatments (Figure 4b).

A significant increase in the N cell quota under HFe conditions and a significant decrease in the P cell quota under LFe conditions were measured with increasing pCO_2 (Figure 5). The cell quota of C, Si, and Chl *a* did not differ significantly with changes in pCO_2 under LFe or HFe conditions (Figure 5). The $In_{cell}[C]$, $In_{cell}[N]$, $In_{cell}[P]$, and $In_{cell}[Chl\ a]$ under HFe conditions increased significantly with increasing pCO_2 (Supplementary Figure S1a–c and e, Table 2). Only $In_{cell}[P]$ decreased significantly with increasing pCO_2 under LFe conditions (Supplementary Figure S1c, Table 2). The [Si]/SA did not differ significantly because of a difference in carbonate chemistry under both LFe and HFe conditions (Supplementary Figure S1d). The NCP, NSiP, and NChl*a*P did not differ significantly among the three xCO_2 treatment in both iron conditions (Supplementary Figure S2a, d, and e). The NNP and NPP under HFe conditions increased significantly with increasing pCO_2 (Table 2), but those trends were not seen under LFe conditions (Supplementary Figure S2b and c). The C:N, C:P, and N:P ratios did not show any significant trends or differences among the three xCO_2 conditions under HFe and LFe conditions (Figure 6a–c). The Si:N, Si:C, and Si:P ratios under HFe conditions decreased significantly with increasing pCO_2, but the ratios did not differ significantly under LFe conditions (Figure 6d–f, Table 2).

Different Fe′ conditions produced significant differences in most of the parameters measured in this study, except for $In_{cell}[P]$, C:N, and Si:P ratios (Table 3). Lower iron availability decreases the cell quota of C and N synchronously. The different iron conditions affected the Si cell quota and Si/SA, but the degree of the change was small compared with the change for C and N, resulting in increasing Si:C and Si:N ratios with increasing iron availability (Table 3). The Chl *a* cell quota, $In_{cell}[Chl\ a]$, and NChl*a*P decreased dramatically with a decrease in iron availability (Supplementary Figure S2, Table 3).

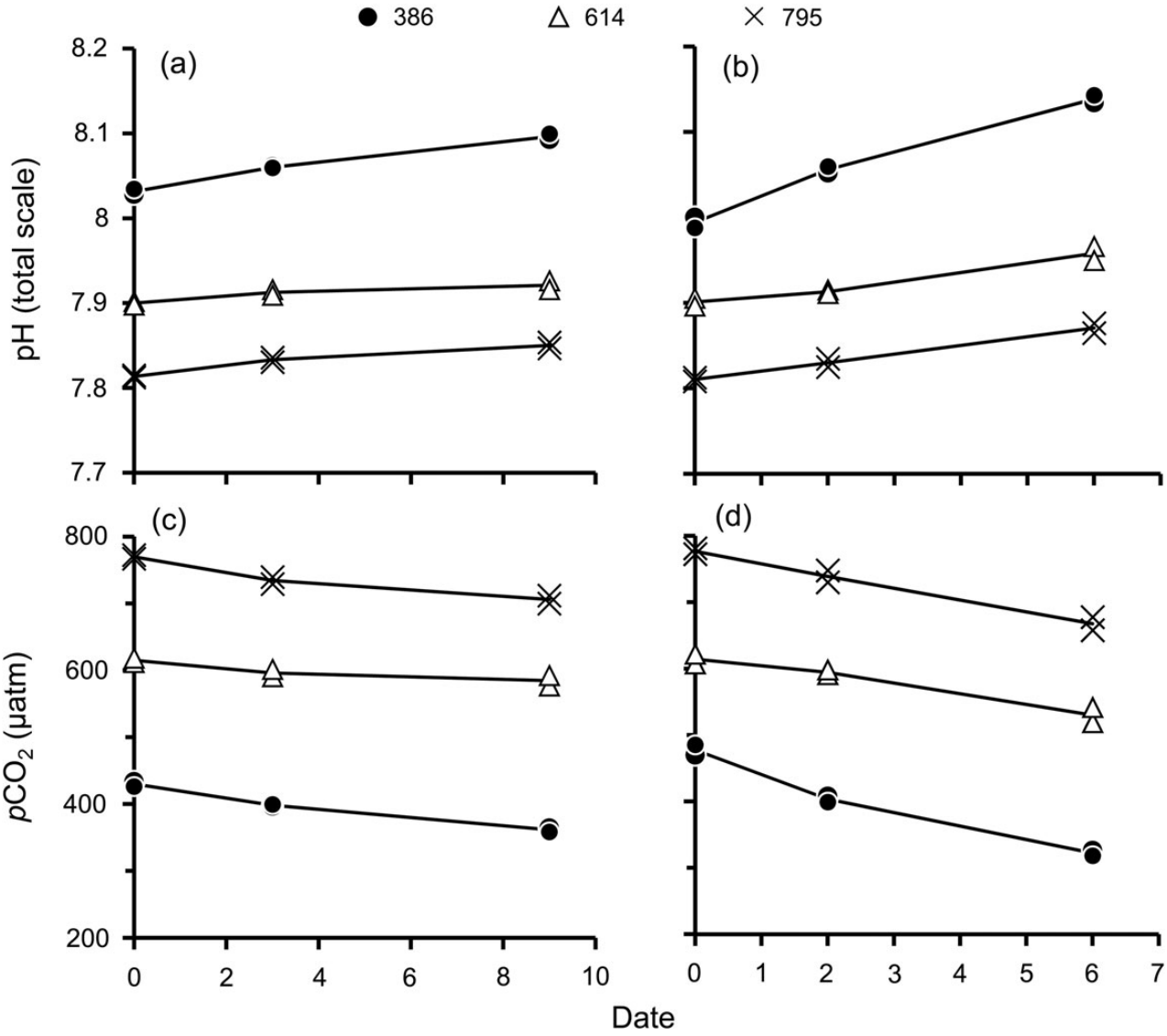

Figure 2. Temporal changes in (a and b) pH (total scale), and (c and d) pCO_2 under LFe (a and c) and HFe (b and d) conditions.

Discussion

This study shows that the cell size and elemental composition of the diatom *T. weissflogii* changed with both separate and simultaneous changes in iron availability and carbonate chemistry. The proper control of bioavailable [Fe′] in seawater under different pCO_2 conditions enables the investigation of individual effects of iron availability and carbonate chemistry on the cellular elemental dynamics of phytoplankton species (Sugie and Yoshimura, 2013). The present study demonstrates that the ecophysiological properties of the coastal and estuary diatom *T. weissflogii* changed in response to the change in CO_2 levels, mainly under iron-replete condition.

Effects of different CO_2 levels on cellular elemental dynamics

Under HFe conditions, $In_{cell}[C]$, $In_{cell}[N]$, $In_{cell}[P]$, and $In_{cell}[Chl\,a]$ increased significantly with increasing pCO_2 (Supplementary Figure S1), suggesting the increasing concentration of intracellular constituents. However, the cell quota of C, P, and Chl *a* did not change (Table 2), because cell size decreased with increasing pCO_2 under HFe conditions. A decrease in cell size in response to high pCO_2 conditions has been reported for micro- and nano-sized phytoplankton such as the diatom *Pseudo-nitzschia pseudodelicatissima* (Sugie and Yoshimura, 2013) and the coccolithophore *Emiliania huxleyi* (Lohbeck *et al.*, 2012). Previous studies have demonstrated that the increase in temperature also decrease cell size of marine phytoplankton ~2.5–4% $°C^{-1}$ (Montagnes and Franklin, 2001; Atkinson *et al.*, 2003). According to the IPCC AR5 (IPCC, 2013), temperature increase in the range 1–3°C (RCP2.6) or 3–10°C (RCP8.5) has been predicted with atmospheric CO_2 concentrations ranging from 421 to 936 ppm by 2100. Such temperature rises could decrease phytoplankton cell size by 2.5 to >40%. Our study estimated the decrease in cell volume to be 1.4×10^{-2}% per pCO_2 increases (Table 2), suggesting that the increase in CO_2 levels in 2100 from the present conditions (~400 µatm) could decrease cell volume by 0.3–7.5% under RCP2.6 and RCP8.6 scenarios, respectively. These estimations suggest that the effect of temperature on cell volume is stronger

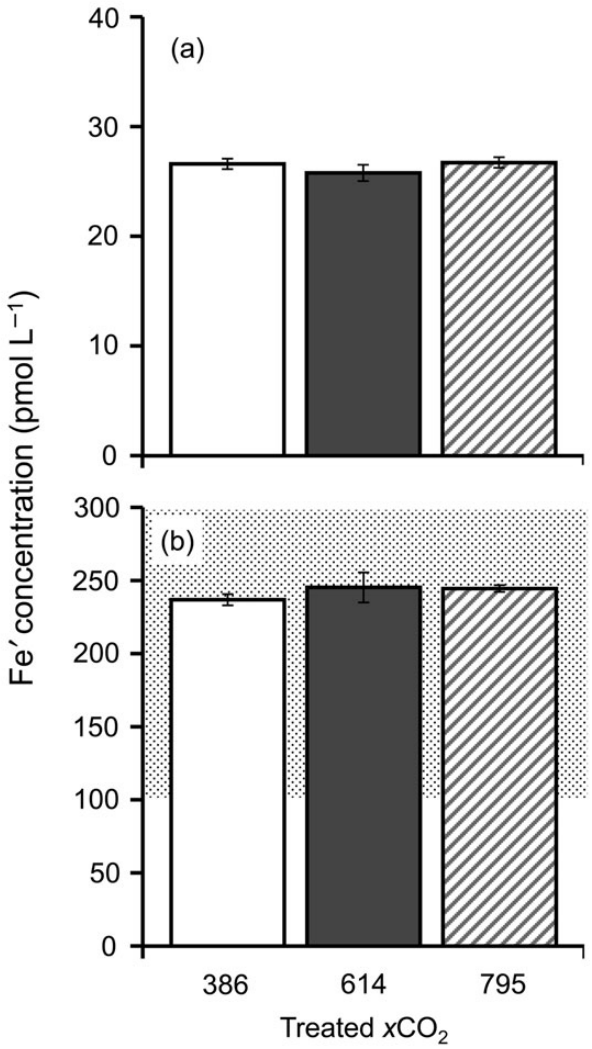

Figure 3. The mean Fe′ concentration under (a) LFe and (b) HFe conditions during the course of the experiment. Error bars represent the range of the values in duplicate incubation bottles. The hatched area indicates where solid iron hydroxides are precipitating.

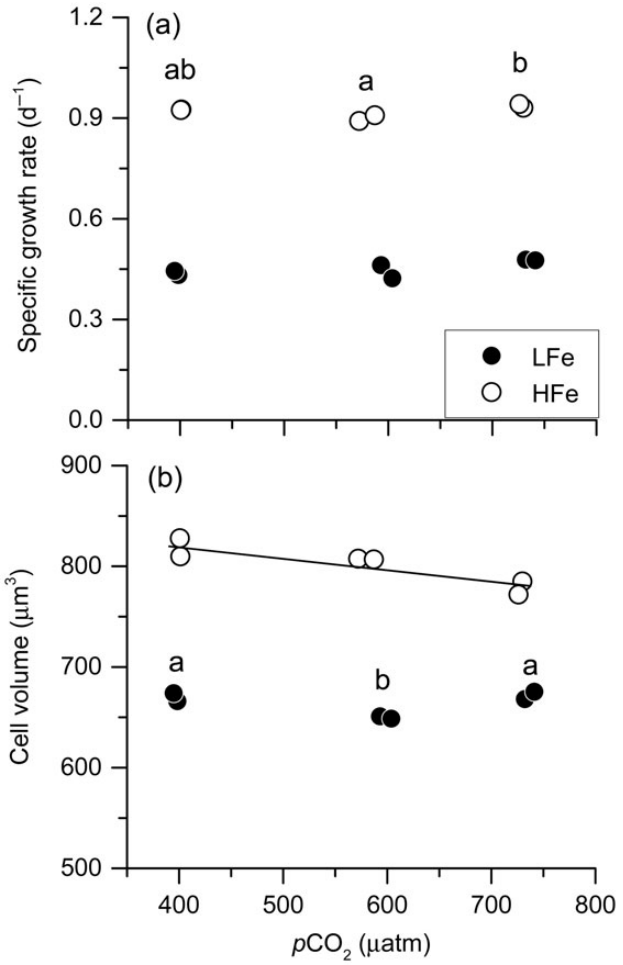

Figure 4. Change in (a) specific growth rate and (b) cell volume of *T. weissflogii* grown under different pCO_2 and iron conditions. The solid line in (b) represents the regression between pCO_2 and cell volume. Statistics are shown in Tables 2 and 3. Labels above the symbols represent the results of Tukey's group test ($p < 0.05$), which did not show a linear trend.

than pCO_2, but pCO_2 increase could contribute substantially (12–19% under RCP2.6 and RCP8.6 scenarios, respectively) to the decrease in cell volume of *T. weissflogii* in the forecasted future conditions, given the decrease in cell size emerge due to the additive effects of hightemperature and pCO_2 under iron-replete conditions. Seebah *et al.* (2014) reported that the aggregate size and sinking velocity of *T. weissflogii* decreased under high pCO_2, which can increase the remineralization of organic matters in the water column. The reduction in cell size found in the present study may partly explain the sinking behaviour of *T. weissflogii* reported by Seebah *et al.* (2014). In addition to the slower sinking rate of *T. weissflogii* under high CO_2 conditions (Seebah *et al.*, 2014), the relatively stable cell quota of C, N, P, and Chl *a* suggest that increasing pCO_2 could have negative impact on the export flux of these bioelements in the high CO_2 conditions.

In contrast, the [Si]/SA and NSiP were not affected significantly by changes in pCO_2 (Table 2). Sugie and Yoshimura (2013) reported that the [Si]/SA and NSiP of *P. pseudodelicatissima* decreased with increasing pCO_2 under various [Fe′] conditions, suggesting that the effect of increasing CO_2 levels is species-specific or differs between centric and pennate diatoms. Milligan *et al.* (2004) examined the Si metabolism of *T. weissflogii* under iron-replete conditions and found that the rates of intracellular Si efflux and frustule dissolution increased in 750 ppm CO_2 compared with 100 ppm CO_2. During that experiment, the Si cell quota did not differ significantly between 380 and 750 ppm CO_2 because of the high Si uptake rate under the high CO_2 conditions. The small but insignificant decrease in [Si]/SA with increasing pCO_2 under LFe conditions may result from the pH-dependent change in Si metabolism as previously reported (Milligan *et al.*, 2004; Hervé *et al.*, 2012). Muggli *et al.* (1996) found that phytoplankton cells suffered from energy limitation under iron-limited conditions. Because Si uptake and mineralization are associated with energy from respiration (Martin-Jézéquel *et al.*, 2000), the [Si]/SA may be slightly affected by changing pCO_2 under conditions of low iron availability.

Effects of different CO_2 levels on elemental compositions

The present study confirms that the cellular C:N, C:P, and N:P ratios do not change with changes in pCO_2 under iron-replete or iron-limited conditions (Figure 6). Previous studies also observed

Table 2. Statistical results of the relationships between partial pressure of CO_2 (pCO_2, μatm) and specific growth rate (μ, d^{-1}), cell volume (CV, μm^3), intracellular organic carbon (In_{cell} [C], mol l^{-1}), intracellular nitrogen (In_{cell} [N], mol l^{-1}), intracellular phosphorus (In_{cell} [P], mol l^{-1}), silicon concentration per unit surface area ([Si]/SA, mmol m^{-2}), intracellular chlorophyll *a* (In_{cell}[Chl-*a*], mg l^{-1}), Net C, N, P, Si, and chlorophyll *a* productions (NCP, NNP, NPP, NSiP, and NChl-*a*P; pmol cell^{-1} d^{-1} for C, N, and Si, and fmol cell^{-1} d^{-1} for P, pg cell^{-1} d^{-1} for chlorophyll *a*), and elemental compositions.

	LFe			HFe		
	a	***b***	**Significance**	***a***	***b***	**Significance**
μ	n.s.	n.s.	n.s.	n.s.	n.s.	n.s.
Cell volume	n.s.	n.s.	n.s.	871**	−0.12*	$F_{1,4} = 15.8$, $p = 0.016$, $R^2 = 0.75$
C quota	n.s.	n.s.	n.s.	n.s.	n.s.	n.s.
N quota	n.s.	n.s.	n.s.	1.2**	2.4×10^{-5}*	$F_{1,4} = 10.4$, $p = 0.032$, $R^2 = 0.65$
P quota	75**	−0.22**	$F_{1,4} = 52.9$, $p = 0.002$, $R^2 = 0.91$	n.s.	n.s.	n.s.
Si quota	n.s.	n.s.	n.s.	n.s.	n.s.	n.s.
Chl *a* quota	n.s.	n.s.	n.s.	n.s.	n.s.	n.s.
In_{cell}[C]	n.s.	n.s.	n.s.	7.8**	2.1×10^{-3}*	$F_{1,4} = 15.7$, $p = 0.017$, $R^2 = 0.75$
In_{cell}[N]	n.s.	n.s.	n.s.	1.3**	5.5×10^{-4}**	$F_{1,4} = 23.4$, $p = 0.008$, $R^2 = 0.82$
In_{cell}[P]	0.12	-3.7×10^{-5}**	$F_{1,4} = 47.8$, $p = 0.002$, $R^2 = 0.90$	0.072**	4.7×10^{-5}*	$F_{1,4} = 12.8$, $p = 0.023$, $R^2 = 0.70$
[Si]/SA	n.s.	n.s.	n.s.	n.s.	n.s.	n.s.
In_{cell}[Chl-*a*]	n.s.	n.s.	n.s.	6.0**	9.5×10^{-4}**	$F_{1,4} = 8.9$, $p = 0.040$, $R^2 = 0.61$
NCP	n.s.	n.s.	n.s.	n.s.	n.s.	n.s.
NNP	n.s.	n.s.	n.s.	1.0**	2.7×10^{-4}*	$F_{1,4} = 12.7$, $p = 0.024$, $R^2 = 0.70$
NPP	n.s.	n.s.	n.s.	58**	0.026*	$F_{1,4} = 8.9$, $p = 0.041$, $R^2 = 0.61$
NSiP	n.s.	n.s.	n.s.	n.s.	n.s.	n.s.
NChl *a*P	n.s.	n.s.	n.s.	n.s.	n.s.	n.s.
C:N	n.s.	n.s.	n.s.	n.s.	n.s.	n.s.
C:P	n.s.	n.s.	n.s.	n.s.	n.s.	n.s.
N:P	n.s.	n.s.	n.s.	n.s.	n.s.	n.s.
Si:N	n.s.	n.s.	n.s.	0.62**	-1.2×10^{-4}**	$F_{1,4} = 29.7$, $p = 0.006$, $R^2 = 0.85$
Si:C	n.s.	n.s.	n.s.	0.11**	-1.1×10^{-5}*	$F_{1,4} = 11.0$, $p = 0.030$, $R^2 = 0.66$
Si:P	n.s.	n.s.	n.s.	11.0**	-3.3×10^{-3}*	$F_{1,4} = 14.0$, $p = 0.020$, $R^2 = 0.72$
C:Chl *a*	n.s.	n.s.	n.s.	n.s.	n.s.	n.s.

Listed are the constant (*a*) and the coefficients (*b*) of regression equation of $y = a + b \times pCO_2$. Asterisks represent the significance level of the constant and coefficients (*$p < 0.05$; **$p < 0.01$; *t*-test, d.f. = 5). n.s., not significant.

that these ratios of *T. weissflogii* were not affected by changes in pCO_2 under both macronutrient-replete and -depleted conditions (Burkhardt *et al.*, 1999; Clark *et al.*, 2014). In the studies by Burkhardt *et al.* (1999) and Clark *et al.* (2014), carbonate chemistry was manipulated by adding acid or base, whereas in the present study, it was manipulated by injecting xCO_2-controlled air. The method of carbonate chemistry manipulation is reported to be one of the most important factors affecting biological responses to ocean acidification (Shi *et al.*, 2009; Hoppe *et al.*, 2011). The major difference between these manipulation methods is DIC concentrations: the bubbling of high CO_2 air increases DIC, whereas the acid/base addition did not change DIC (Burkhardt *et al.*, 2001; Shi *et al.*, 2009). Taken together, the present and previous findings indicate that increasing CO_2 levels have no effect on the C:N, C:P, and N:P ratios of *T. weissflogii*, irrespective of the different manipulation methods.

However, some previous studies have reported that cellular C:P and N:P ratios of phytoplankton are affected by increases in pCO_2 under iron-replete conditions. Many centric and pennate diatom species showed an increase in C:P ratio in response to increases in pCO_2 (Burkhardt *et al.*, 1999; King *et al.*, 2011; Sun *et al.*, 2011; Sugie and Yoshimura, 2013). An increase in the C:P ratio with increasing pCO_2 has also been found in Dinophyceae, Raphidophyceae, and Prymnesiophyceae (Feng *et al.*, 2008; Fu *et al.*, 2008). Some diatom species such as *Asteionellopsis glacialis* and *Phaeodactylum tricornutum* did not show changes in the C:P ratio with changing pCO_2 (Burkhardt *et al.*, 1999), similar to the finding for *T. weissflogii* in the present study. Sugie and Yoshimura (2013) demonstrated using *P. pseudodelicatissima* that a steeper decline in In_{cell}[P] and NPP compared with those of C and N with increasing pCO_2 is a key mechanism underlying increasing C:P and N:P ratios in high CO_2 conditions. They suggested that increases in C:P and N:P ratios with increasing CO_2 availability were derived from decreases in the expenditure of P-rich cellular constituents such as ATP, which is used to maintain/operate carbon concentration mechanisms (CCMs; Hopkinson *et al.*, 2011). A notable characteristic of C assimilation in *T. weissflogii* is the presence of both C_3 and C_4 photosynthetic pathways, where the latter functions as a biochemical CCM. In contrast, other diatoms are mainly C_3 photosynthesizers (Roberts *et al.*, 2007). The initial products of DIC uptake are glycerate-P and hexose-P in C_3 diatoms, and malate in C_4 diatoms of *T. weissflogii* (Roberts *et al.*, 2007). If C_4 pathway-mediated CCMs decrease with increasing CO_2 availability, the contribution of sugar-P compounds such as glycerate-P mediated from C_3 photosynthesis can increase with increasing CO_2 availability. Such adaptive photosynthetic strategies result in an increase in NPP (Supplementary Figure S2), which could offset increases in C:P and N:P ratios of *T. weissflogii* with increasing pCO_2.

In contrast to the relatively stable C:N, C:P, and N:P ratios in the present study, we found that the ratios of Si to C, N, and P changed in response to changes in carbonate chemistry (Figure 6). This discrepancy reflected different trends in the effect of pCO_2 on the rates of NEP between Si and C, N, and P (Supplementary Figure S2). Under HFe conditions, the decrease in Si:N and Si:P with increasing pCO_2 was derived from the significant increases in NNP and NPP with increasing pCO_2. The decreasing trend of Si:C with increasing pCO_2 resulted from the small but insignificant ($p = 0.16$, ANOVA)

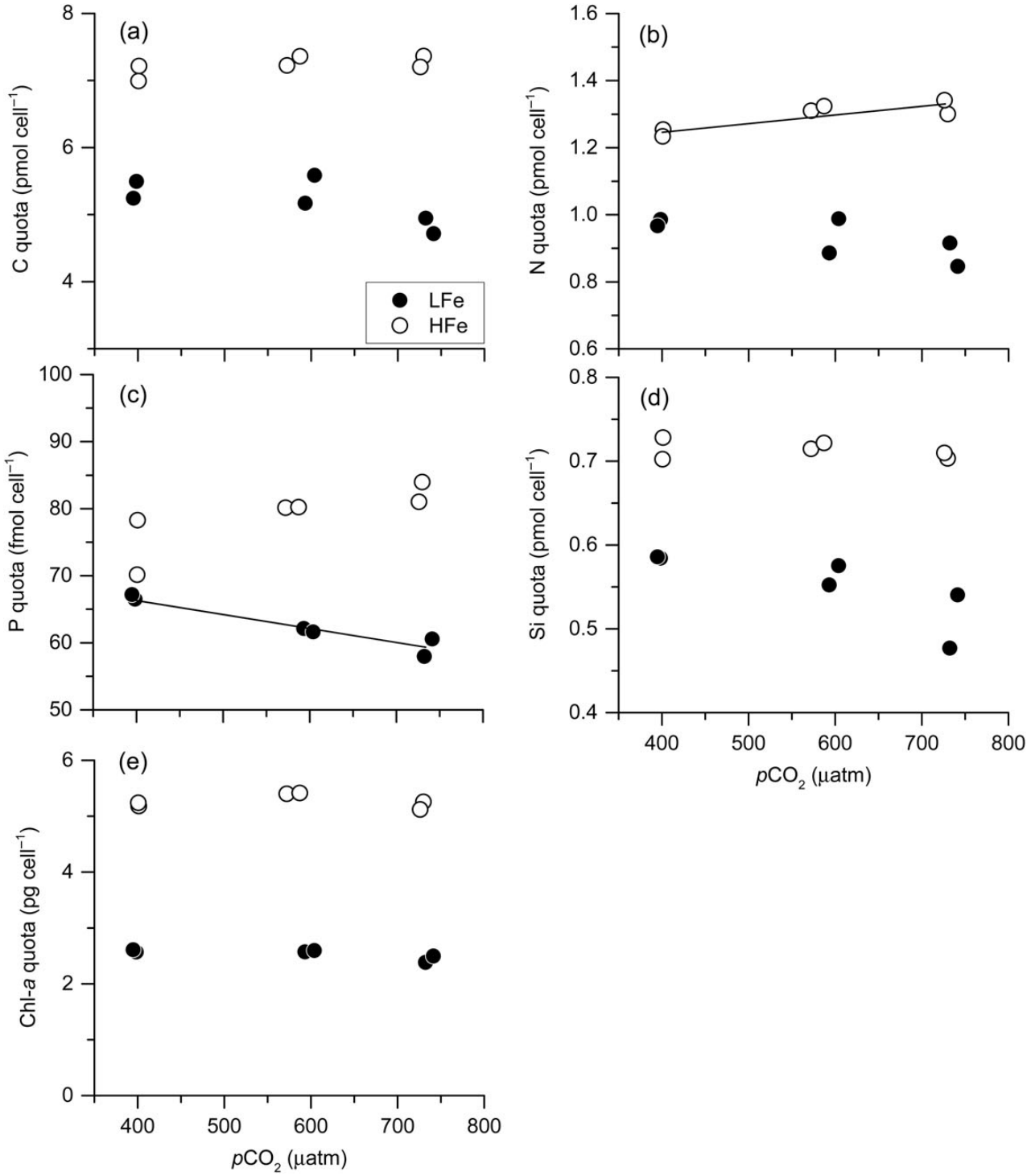

Figure 5. Changes in the cell quota of (a) carbon, (b) nitrogen, (c) phosphorus, (d) silicon, and (e) chlorophyll *a* of *T. weissflogii* grown under different pCO_2 and iron conditions. Solid lines in (b) and (c) represent the regression between pCO_2 and N and P cell quota, respectively. Statistics are shown in Tables 2 and 3.

increase in NCP and constant NSiP with increasing pCO_2. Decreasing Si relative to C, N, and P in response to increasing pCO_2 has been previously reported for diatoms (*Pseudo-nitzschia multiseries*, Sun *et al.*, 2011; *P. pseudodelicatissima*, Sugie and Yoshimura, 2013). It has also been reported that cell cycle-dependent uptake of Si and C, N, and P were uncoupled (Claquin *et al.*, 2002). The present results further support such uncoupling and indicate that ratios of Si to other nutrients in diatoms can change in response to changes in environmental conditions including carbonate chemistry.

Under LFe conditions, elemental compositions did not differ significantly among the three pCO_2 conditions because of constant

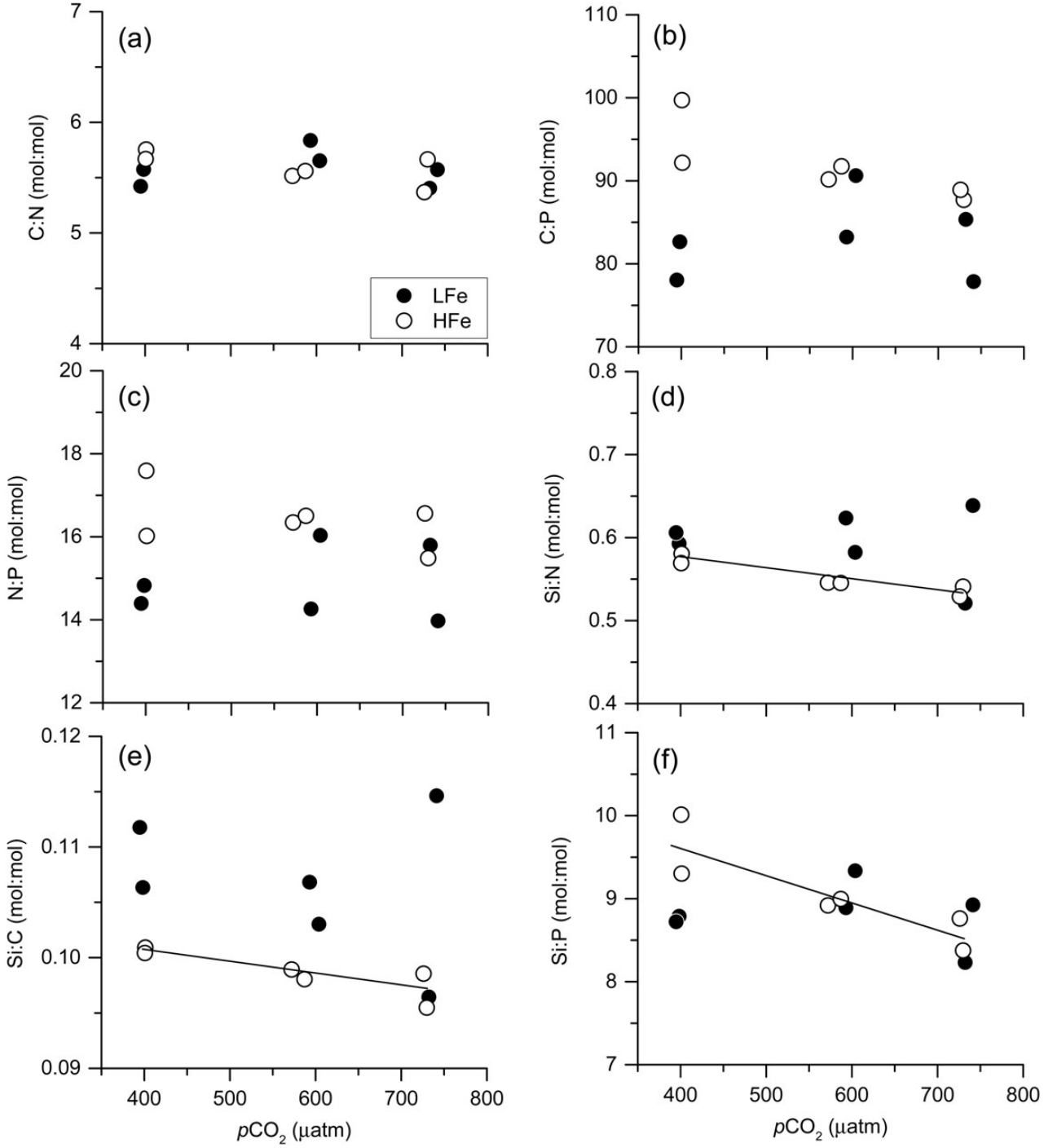

Figure 6. Change in (a) C:N, (b) C:P, (c) N:P, (d) Si:N, (e) Si:C, and (f) Si:P ratios of *T. weissflogii* grown under different pCO_2 and iron conditions. Solid lines in (d–f) represent the significant regressions between pCO_2 and Si:N, Si:C, and Si:P ratios, respectively. Statistics are shown in Tables 2 and 3.

NCP, NNP, NPP, and NSiP (Supplementary Figure S2), which are clearly different from the results obtained in the HFe conditions (Figure 6). This discrepancy may be caused by unexplored physiological mechanisms. We assume that the processes responsible for the increase in NEP with increasing pCO_2 as was found in the HFe conditions require additional energy for nutrient uptake. Under the energy-limited LFe conditions (Muggli *et al.*, 1996), the CO_2-related change in NEP was regulated by the iron-limitation. Hoppe *et al.* (2013) also observed that the effects of high CO_2 conditions on natural phytoplankton communities in the Southern Ocean were minimal under iron-depleted (siderophore desferrioxamine B added) conditions compared with iron-replete conditions. However, the rates of change in NEP of the diatom *P. pseudodelicatissima* were affected by changes in pCO_2 under conditions of low iron availability (Sugie and Yoshimura, 2013). The notable difference between *T. weissflogii* and *P. pseudodelicatissima* is k_μ value that *T. weissflogii* and *P. pseudodelicatissima* showed $k_\mu = 28$ and 1.5–5.0 pmol [Fe′] l^{-1}, respectively. These results

Table 3. Results of two-tailed, paired-sample *t*-test ($n = 12$) to test the effect of iron availability on the measured parameters, comparing the LFe ($Fe' = \sim 26$ pmol l^{-1}) and the HFe treatments ($Fe' = \sim 240$ pmol l^{-1}).

	Effect of decreasing Fe′	*p*-value
μ	Decrease	<0.001
Cell volume	Decrease	<0.001
C quota	Decrease	<0.001
N quota	Decrease	<0.001
P quota	Decrease	<0.001
Si quota	Decrease	<0.001
Chl *a* quota	Decrease	<0.001
$\ln_{cell}$[C]	Decrease	0.009
$\ln_{cell}$[N]	Decrease	0.018
$\ln_{cell}$[P]	n.s.c.	0.526
$\ln_{cell}$[Chl *a*]	Decrease	<0.001
Si/SA	Decrease	0.010
NCP	Decrease	<0.001
NNP	Decrease	<0.001
NPP	Decrease	<0.001
NSiP	Decrease	<0.001
NChl *a*P	Decrease	<0.001
C:N	n.s.c.	0.914
C:P	Decrease	0.034
N:P	Decrease	0.037
Si:N	Increase	0.045
Si:C	Increase	0.016
Si:P	n.s.c.	0.354
C:Chl *a*	Increase	<0.001

Three CO_2 treatments were pooled in LFe and HFe treatments, respectively. n.s.c., not significant change.

indicate that responses to the interaction between changes in pCO_2 and changes in iron availability vary among species depending on the affinity for uptake of [Fe′]. Previous studies have reported that the elemental composition of diatoms is not always related linearly to iron availability (Price, 2005; Bucciarelli *et al.*, 2010). More experiments manipulating various Fe′ and pCO_2 conditions using more phytoplankton species are required to better understand the effect of different CO_2 conditions on biogeochemical cycling of bioelements.

Effect of different iron availability on ecophysiology of *T. weissflogii*

Decreasing iron availability affected most of the measured parameters of *T. weissflogii*, indicating that iron availability is more important to determine ecophysiological processes of diatoms than variations in carbonate chemistry. Yoshimura *et al.* (2014) also suggested that changes in pCO_2 do not play a major role in the dynamics of particulate and dissolved organic matter produced by subarctic plankton communities during the exponential growth phase. Price (2005) reported that the C:N:Si:P ratio of *T. weissflogii* changed from 97:14:4.7:1 to 70:10:5.9:1 under iron-replete and iron-limited conditions, respectively. In the present study, we obtained similar results under HFe (96:17:9.7:1) and LFe (80:15:8.8:1) conditions in the 386 ppm xCO_2 treatments. By calculating Q_E ratios (RQ_E) between LFe386 and HFe386 ($RQ_E = Q_{E\text{-}LFe}/Q_{E\text{-}HFe}$, where $Q_{E\text{-}LFe}$ and $Q_{E\text{-}HFe}$ represent cell quota of each element in LFe386 and HFe386 treatment, respectively), we obtained 0.76, 0.78, 0.90, and 0.82 for RQ_C, RQ_N, RQ_P, and RQ_{Si}, respectively (Supplementary Figure S3). This estimate suggests that Q_C, Q_N, and Q_{Si} are highly variable compared with Q_P in response to the different iron conditions. In addition, the changes in carbonate chemistry modulated the elemental composition of *T. weissflogii* possibly via uncoupling of the cell cycle-dependent uptake of each bioelement (Claquin *et al.*, 2002). Specifically, the difference in the Si:N ratio between HFe and LFe conditions increased with increasing pCO_2 (Figure 6d). Such unexplored flexible nutrient stoichiometry may be a consequence of optimality of nutrient uptake or assimilations (Milligan *et al.*, 2004; Smith *et al.*, 2011), the mechanisms of which should be incorporated into the model simulations to better predict the biogeochemical cycling of nutrients.

Relevance of this study for ocean acidification study

Results of our short-term experiment contribute to better understanding of first-order biogeochemical processes of nutrients in dynamic coastal environment, but the progress of ocean acidification in nature is a slower process compared with our short-term experiment. Extrapolating our results to the future acidified environment require attention because long-term adaptive responses often differ from short-term phenotypic plasticity (Lohbeck *et al.*, 2012; Collins *et al.*, 2014). Crawfurd *et al.* (2011) and Tatters *et al.* (2013) reported that there was no clear difference in the effect of high CO_2 conditions on the ecophysiology of diatoms, when comparing the results of short-term plastic response with acclimation/adaptation responses for >100 cell divisions. On the other hand, Torstensson *et al.* (2015) reported that the specific growth rate decreased in the high CO_2 conditions only after the acclimation of ~60 cell divisions. Because phenotypic plasticity may be important for the subsequent adaptation or evolution of organisms (Collins *et al.*, 2014), plastic response found in this study could provide relevant information for the future acidified ocean ecosystem. However, there is very limited information available to date concerning adaptation of diatoms, and no reports are available on the adaptive response of cell size and cellular elemental content of diatoms. We need more information on the long-term effect of CO_2 on phytoplankton ecophysiology.

Conclusions

Our study demonstrated that some ecophysiological properties of coastal diatom *T. weissflogii* changed in response to changing CO_2 levels under iron-replete conditions. In coastal environment, iron concentration is generally higher than the oceanic region (Kuma *et al.*, 2000; Nishioka *et al.*, 2013; Bundy *et al.*, 2015), suggesting the change in the ecophysiological properties of *T. weissflogii* could occur with increasing CO_2 levels in the modern coastal seas (Wootton *et al.*, 2008). These changes may affect the food availability of higher trophic levels, sinking behaviour of *T. weissflogii*, and nutrient availability for other phytoplankton in the coastal regions. However, in addition to the differences in the response of individual phytoplankton species to changes in CO_2 levels (e.g. Doney *et al.*, 2009; Collins *et al.*, 2014), previous studies of the impacts of increasing CO_2 levels on the elemental composition of natural plankton communities have produced conflicting results, including no effect (Martin and Tortell, 2006; Feng *et al.*, 2010; Tortell *et al.*, 2010), increased particulate Si:N and Si:C ratios (Sugie *et al.*, 2013), and inconsistent changes in the production of dissolved and particulate organic matters (Yoshimura *et al.*, 2010, 2013, 2014). To interpret these results, it is necessary to improve knowledge of the effects of carbonate chemistry and iron availability on phytoplankton processes using both natural phytoplankton communities and laboratory-based unialgal cultures.

Supplementary data

Supplementary material is available at the *ICESJMS* online version of the manuscript.

Acknowledgements

We acknowledge three anonymous reviewers for providing valuable comments, which significantly improved the paper. The iron data in the medium were kindly provided by Dr J. Nishioka of Hokkaido University. We also thank K. Sugita, A. Tsuzuku, and N. Kageyama for their help on maintaining our culture collection of marine phytoplankton. This work was conducted in the framework of the Plankton Ecosystem Response to CO_2 Manipulation Study (PERCOM) project and supported by the grants from CRIEPI (#060215) and Grants-in-Aid for Scientific Research (#22681004) and by the Japan Agency for Marine-Earth Science and Technology (JAMSTEC).

References

Atkinson, D., Ciotti, B. J., and Montagnes, D. J. S. 2003. Protists decrease in size linearly with temperature: *ca*. 2.5% $^{\circ}C^{-1}$. Proceedings of Royal Society London, Series B, 270: 2605–2611.

Bucciarelli, E., Pondaven, P., and Sarthou, G. 2010. Effects of an iron-light co-limitation on the elemental composition (Si, C, N) of the marine diatoms *Thalassiosira oceanica* and *Ditylum brightwellii*. Biogeosciences, 7: 657–669.

Bundy, R. M., Abdulla, H. A. N., Hatcher, P. G., Biller, D. V., Buck, K. N., and Barbeau, K. A. 2015. Iron-binding ligands and humic substances in the San Francisco Bay estuary and estuarine-influenced shelf regions of coastal California. Marine Chemistry, 173: 183–194.

Burkhardt, S., Amoroso, G., Riebesell, U., and Sültemeyer, D. 2001. CO_2 and HCO_3^- uptake in marine diatoms acclimated to different CO_2 concentrations. Limnology and Oceanography, 46: 1378–1391.

Burkhardt, S., Zondervan, I., and Riebesell, U. 1999. Effect of CO_2 concentration on C:N:P ratio in marine phytoplankton: a species comparison. Limnology and Oceanography, 44: 683–690.

Claquin, P., Martin-Jézéquel, V., Kromkamp, J. C., Veldhuis, M. J. W., and Kraay, G. W. 2002. Uncoupling of silicon compared with carbon and nitrogen metabolisms and the role of the cell cycle in continuous culture of *Thalassiosira pseudonana* (Bacillariophyceae) under light, nitrogen, and phosphorus control. Journal of Phycology, 38: 922–930.

Clark, D. R., Flynn, K. J., and Fabian, H. 2014. Variation in elemental stoichiometry of the marine diatom *Thalassiosira weissflogii* (Bacillariophyceae) in response to combined nutrient stress and changes in carbonate chemistry. Journal of Phycology, 50: 640–651.

Collins, S., Rost, B., and Rynearson, T. A. 2014. Evolutionary potential of marine phytoplankton under ocean acidification. Evolutionary Applications, 7: 140–155.

Crawfurd, K. J., Raven, J. A., Wheeler, G. L., Baxter, E. J., and Joint, I. 2011. The response of *Thalassiosira pseudonana* to long-term exposure to increased CO_2 and decreased pH. PLoS ONE, 6: e26695.

Doney, S. C., Fabry, V. J., Feely, R. A., and Kleypas, J. A. 2009. Ocean acidification: the other CO_2 problem. Annual Review of Marine Science, 1: 169–192.

Dore, J. E., Lukas, R., Sadler, D. W., Church, M. J., and Karl, D. M. 2009. Physical and biogeochemical modulation of ocean acidification in the central North Pacific. Proceedings of the National Academy of Sciences of the United States of America, 106: 12235–12240.

Edmond, J. W. 1970. High precision determination of titration alkalinity and total carbon dioxide content of seawater by potentiometric titration. Deep-Sea Research, 17: 737–750.

Eggers, S. L., Lewandowska, A. M., Barcelos e Ramos, J., Blanco-Ameijeiras, S., Gallo, F., and Matthiessen, B. 2014. Community composition has greater impact on the functioning of marine phytoplankton communities than ocean acidification. Global Change Biology, 20: 713–723.

Feng, Y., Hare, C. E., Rose, J. M., Handy, S. M., DiTullio, G. R., Lee, P. A., Smith, W. O., Jr., *et al.* 2010. Interactive effects of iron, irradiance and CO_2 on Ross Sea phytoplankton. Deep Sea Research I, 57: 368–383.

Feng, Y., Warner, M. E., Zhang, Y., Sun, J., Fu, F. X., Rose, J. M., and Hutchins, D. A. 2008. Interactive effects of increased pCO_2, temperature and irradiance on the marine coccolithophore *Emiliania huxleyi* (Prymnesiophyceae). European Journal of Phycology, 43: 87–98.

Fu, F. X., Zhang, Y., Warner, M. E., Feng, Y., Sun, J., and Hutchins, D. A. 2008. A comparison of future increased CO_2 and temperature effects on sympatric *Heterosigma akashiwo* and *Prorocentrum minimum*. Harmful Algae, 7: 76–90.

Geider, R. J., La Roche, J., Greene, R. M., and Olaizola, M. 1993. Response of the photosynthetic apparatus of *Phaeodactylum tricornutum* (Bacillariophyceae) to nitrate, phosphate, or iron starvation. Journal of Phycology, 29: 755–766.

Hassler, C. S., Schoemann, V., Nichols, C. M., Butler, E. C. V., and Boyd, P. W. 2011. Saccharides enhance iron bioavailability to Southern Ocean phytoplankton. Proceedings of the National Academy of Sciences of the United States of America, 108: 1076–1081.

Hervé, V., Derr, J., Douady, S., Quinet, M., Moisan, L., and Lopez, P. L. 2012. Multiparametric analysis reveal the pH-dependence of silicon biomineralization in diatoms. PLoS ONE, 7: e46722.

Hopkinson, B. M., Dupont, C. L., Allen, A. E., and Morel, F. M. M. 2011. Efficiency of the CO_2-concentrating mechanism of diatoms. Proceedings of the National Academy of Sciences of the United States of America, 108: 3830–3837.

Hoppe, C. J. M., Hassler, C. S., Payne, C. D., Tortell, P. D., Rost, B., and Trimborn, S. 2013. Iron limitation modulates ocean acidification effects on Southern Ocean phytoplankton communities. PLoS ONE, 8: e79890.

Hoppe, C. J. M., Langer, G., and Rost, B. 2011. *Emiliania huxleyi* shows identical response to elevated pCO_2 in TA and DIC manipulations. Journal of Experimental Marine Biology and Ecology, 406: 54–62.

IGBP, IOC, and SCOR. 2013. Ocean acidification summary for policymakers—Third Symposium on the Ocean in a High-CO_2 World. International Geosphere-Biospere Programme, Stockholm, Sweden.

IPCC. 2013. Summary for policymakers. *In* Climate Change 2013: the Physical Science Basis. Contribution of Working Group I to the Fifth Assessment Report of the Intergovernmental Panel on Climate Change. Ed. by T. F. Stocker, D. Qin, G-K. Plattner, M. Tignor, S. K. Allen, J. Boschung, A. Nauels, *et al.* Cambridge University Press, Cambridge, UK and New York, USA.

King, A. L., Sañudo-Wilhelmy, S. A., Leblanc, K., Hutchins, D. A., and Fu, F. 2011. CO_2 and vitamin B_{12} interactions determine bioactive trace metal requirements of a subarctic Pacific diatom. The ISME Journal, 5: 1388–1396.

Kuma, K., Katsumoto, A., Shiga, N., Sawabe, T., and Matsunaga, K. 2000. Variation of size-fractionated Fe concentrations and Fe(III) hydroxide solubilities during a spring phytoplankton bloom in Funka Bay (Japan). Marine Chemistry, 71: 111–123.

Laglera, L. M., and van den Berg, C. M. G. 2009. Evidence for geochemical control of iron by humic substances in seawater. Limnology and Oceanography, 54: 610–619.

LaRoche, J., Rost, B., and Engel, A. 2011. Bioassays, batch culture and chemostat experimentation. *In* Guide to Best Practices for Ocean Acidification Research and Data Reporting, pp. 81–94. Ed. by U. Rievesell, V. J. Fabry, L. Hansson, and J. P. Gattuso. Publications Office of the European Union, Luxembourg. 260 pp.

Lewis, E., and Wallance, D. W. R. 1998. Program developed for CO_2 system calculations. ORNL/CDIAC-105. Carbon Dioxide Information Analysis Center, Oak Ridge National Laboratory, US Department of Energy, Oak Ridge, TN.

Lohbeck, K. T., Riebesell, U., and Reusch, T. B. H. 2012. Adaptive evolution of a key phytoplankton species to ocean acidification. Nature Geoscience, 5: 346–351.

Martin, C. L., and Tortell, P. D. 2006. Bicarbonate transport and extracellular carbonic anhydrase activity in Bering Sea phytoplankton assemblages: results from isotope disequilibrium experiments. Limnology and Oceanography, 51: 2111–2121.

Martin-Jézéquel, V., Hildebrand, M., and Brzezinski, M. A. 2000. Silicon metabolism in diatom: implications for growth. Journal of Phycology, 36: 821–840.

Millero, F. J., Woosley, R., DiTrolio, B., and Waters, J. 2009. Effect of ocean acidification on the speciation of metals in seawater. Oceanography, 22: 72–85.

Milligan, A. J., Varela, D. E., Brzezinski, M. A., and Morel, F. M. M. 2004. Dynamics of silicon metabolism and silicon isotopic discrimination in a marine diatom as a function of pCO_2. Limnology and Oceanography, 49: 322–329.

Montagnes, D. J. S., and Franklin, D. J. 2001. Effect of temperature on diatom volume, growth rate, and carbon and nitrogen content: reconsidering some paradigms. Limnology and Oceanography, 46: 2008–2018.

Morel, F. M. M., Kustka, A. B., and Shaked, Y. 2008. The role of unchelated Fe in the iron nutrition of phytoplankton. Limnology and Oceanography, 53: 400–403.

Muggli, D. L., Lecourt, M., and Harrison, P. J. 1996. Effects of iron and nitrogen source on the sinking rate, physiology and metal composition of an oceanic diatom from the subarctic Pacific. Marine Ecology Progress Series, 132: 215–227.

Nishioka, J., Nakatsuka, T., Watanabe, Y. W., Yasuda, I., Kuma, K., Ogawa, H., Ebuchi, N., *et al.* 2013. Intensive mixing along an island chain controls oceanic biogeochemical cycles. Global Biogeochemical Cycles, 27: 1–10.

Obata, H., Karatani, H., and Nakayama, E. 1993. Automated determination of iron in seawater by chelating resin concentration and chemiluminescence detection. Analitycal Chemistry, 65: 1524–1528.

Paasche, E. 1980. Silicon content of five marine plankton diatom species measured with a rapid filter method. Limnology and Oceanography, 25: 474–480.

Passow, U., and Carlson, C. A. 2012. The biological pump in a high CO_2 world. Marine Ecology Progress Series, 249: 249–271.

Price, N. M. 2005. The elemental stoichiometry and composition of an iron-limited diatom. Limnology and Oceanography, 50: 1159–1171.

Price, N. M., Harrison, G. I., Hering, J. G., Hudson, R. J. M., Nirel, P. M. V., Palenik, B. P., and Morel, F. M. M. 1988/1989. Preparation and chemistry of the artificial algal culture medium Aquil. Biological Oceanography, 6: 443–461.

Quigg, A., Finkel, Z. V., Irwwin, A. J., Rosenthal, Y., Ho, T. Y., Reinfelder, J. R., Schofield, O., *et al.* 2003. The evolutionary inherence of elemental stoichiometry in marine phytoplankton. Nature, 425: 291–293.

Raven, J. A., Evans, M. C. W., and Korb, R. E. 1999. The role of trace metals in photosynthetic electron transport in O_2-evolving organisms. Photosynthesis Research, 60: 111–149.

Richier, S., Achterberg, E. P., Dumousseaud, C., Poulton, A. J., Suggett, D. J., Tyrrell, T., Zubkov, M. V., *et al.* 2014. Phytoplankton responses and associated carbon cycling during shipboard carbonate chemistry manipulation experiments conducted around Northwest European shelf seas. Biogeosciences, 11: 4733–4752.

Roberts, K., Granum, E., Leegood, R. C., and Raven, J. A. 2007. C3 and C4 pathways of photosynthetic carbon assimilation in marine diatoms are under genetic, not environmental, control. Plant Physiology, 145: 230–235.

Seebah, S., Fairfield, C., Ullrich, M. S., and Passow, U. 2014. Aggregation and sedimentation of *Thalassiosira weissflogii* (diatom) in a warmer and more acidified future ocean. PLoS ONE, 9: e112379.

Shi, D., Xu, Y., Hopkinson, B. M., and Morel, F. M. M. 2010. Effect of ocean acidification on iron availability to marine phytoplankton. Science, 327: 676–679.

Shi, D., Xu, Y., and Morel, F. M. M. 2009. Effects of the pH/pCO_2 control method on medium chemistry and phytoplankton growth. Biogeosciences, 6: 1199–1207.

Smith, S. L., Pahlow, M., Merico, A., and Wirtz, K. W. 2011. Optimality-based modeling of planktonic organisms. Limnology and Oceanography, 56: 2080–2094.

Solórzano, L., and Sharp, J. H. 1980. Determination of total dissolved phosphorus and particulate phosphorus in natural waters. Limnology and Oceanography, 25: 754–758.

Stumm, W., and Morgan, J. J. 1996. Aquatic Chemistry, 3rd edn. Wiley Interscience, New York.

Sugie, K., Endo, H., Suzuki, K., Nishioka, J., Kiyosawa, H., and Yoshimura, T. 2013. Synergistic effects of pCO_2 and iron availability on nutrient consumption ratio of the Bering Sea phytoplankton community. Biogeosciences, 10: 6309–6321.

Sugie, K., Kuma, K., Fujita, S., and Ikeda, T. 2010. Increase in Si:N drawdown ratio due to resting spore formation by spring bloom-forming diatoms under Fe- and N-limited conditions in the Oyashio region. Journal of Experimental Marine Biology and Ecology, 382: 108–116.

Sugie, K., and Yoshimura, T. 2013. Effects of pCO_2 and iron on the elemental composition and cell geometry of the marine diatom *Pseudo-nitzschia pseudodelicatissima*. Journal of Phycology, 49: 475–488.

Sun, J., Hutchins, D. A., Feng, Y., Seubert, E. L., Caron, D. A., and Fu, F. X. 2011. Effects of changing pCO_2 and phosphate availability on domoic acid production and physiology of the marine harmful bloom diatom *Pseudo-nitzschia multiseries*. Limnology and Oceanography, 56: 829–840.

Sunda, W., and Huntsman, S. 2003. Effect of pH, light, and temperature on Fe-EDTA chelation and Fe hydrolysis in seawater. Marine Chemistry, 84: 35–47.

Sunda, W. G., and Huntsman, S. A. 1995. Iron uptake and growth limitation in oceanic and coastal phytoplankton. Marine Chemistry, 50: 189–206.

Suzuki, R., and Ishimaru, T. 1990. An improved method for the determination of phytoplankton chlorophyll using N, N-dimethylformamide. Journal of Oceanographic Society of Japan, 46: 190–194.

Takeda, S. 1998. Influence of iron availability on nutrient consumption ratio of diatoms in oceanic waters. Nature, 393: 774–777.

Tatters, A. O., Roleda, M. Y., Schnetzer, A., Fu, F., Hurd, C. L., Boyd, P. W., and Caron, D. A., et al. 2013. Short- and long-term conditioning of a temperate marine diatom community to acidification and warming. Philosophical Transactions of the Royal Society B, 368: 20120437.

Torstensson, A., Hedblom, M., Björk, M. M., Chierici, M., and Wulff, A. 2015. Long-term acclimation to elevated pCO_2 alters carbon metabolism and reduces growth in the Antarctic diatom *Nitzschia lecointei*. Proceedings of the Royal Society B, 282: 20151513.

Tortell, P. D., Trimborn, S., Li, Y., Rost, B., and Payne, C. D. 2010. Inorganic carbon utilization by Ross Sea phytoplankton across natural and experimental CO_2 gradients. Journal of Phycology, 46: 433–443.

Weber, T. S., and Deutsch, C. 2010. Ocean nutrient ratios governed by phytoplankton biogeography. Nature, 467: 550–554.

Welschmeyer, N. A. 1994. Fluorometric analysis of chlorophyll *a* in the present of chlorophyll *b* and pheopigments. Limnology and Oceanography, 39: 1985–1992.

Wootton, J. T., Pfister, C. A., and Forester, J. D. 2008. Dynamic patterns and ecological impacts of declining ocean pH in a high-resolution multi-year dataset. Proceedings of the National Academy of Sciences of the United States of America, 105: 18848–18853.

Yoshimura, T., Nishioka, J., Suzuki, K., Hattori, H., Kiyosawa, H., and Watanabe, W. Y. 2010. Impacts of elevated CO_2 on organic carbon dynamics in nutrient depleted Okhotsk Sea surface waters. Journal of Experimental Marine Biology and Ecology, 395: 191–198.

Yoshimura, T., Sugie, K., Endo, H., Suzuki, K., Nishioka, J., and Ono, T. 2014. Organic matter production response to CO_2 increase in open subarctic plankton communities: comparison of six microcosm experiments under iron-limited and -enriched conditions. Deep Sea Research I, 94: 1–14.

Yoshimura, T., Suzuki, K., Kiyosawa, H., Ono, T., Hattori, H., Kuma, K., and Nishioka, J. 2013. Impacts of elevated CO_2 on particulate and dissolved organic matter production: microcosm experiments using iron deficient plankton communities in open subarctic waters. Journal of Oceanography, 69: 601–618.

Handling editor: Shubha Sathyendranath